10.1063/1.347181

Growth of native oxide on a silicon surface

M. Morita, T. Ohmi, E. Hasegawa, M. Kawakami,[a] and M. Ohwada[b]
Department of Electronics, Faculty of Engineering, Tohoku University, Sendai 980, Japan

(Received 19 December 1989; accepted for publication 30 March 1990)

The control factors controlling the growth of native silicon oxide on silicon (Si) surfaces have been identified. The coexistence of oxygen and water or moisture is required for growth of native oxide both in air and in ultrapure water at room temperature. Layer-by-layer growth of native oxide films occurs on Si surfaces exposed to air. Growth of native oxides on *n*-Si in ultrapure water is described by a parabolic law, while the native oxide film thickness on n^+-Si in ultrapure water saturates at 10 Å. The native oxide growth on *n*-Si in ultrapure water is continuously accompanied by a dissolution of Si into the water and degrades the atomic flatness at the oxide-Si interface, producing a rough oxide surface. A dissolution of Si into the water has not been observed for the Si wafer having surface covered by the native oxide grown in air. Native oxides grown in air and in ultrapure de-ionized water have been demonstrated experimentally to exhibit remarkable differences such as contact angles of ultrapure water drops and chemical binding energy. These chemical bond structures for native oxide films grown in air and in ultrapure water are also discussed.

I. INTRODUCTION

The control of native oxide growth rate on Si surfaces is of great importance in the fabrication of ultralarge-scale integrated devices. Native oxide films on Si surfaces prevent the low-temperature growth of high-quality epitaxial Si films and precise control of the thickness and electrical properties of very-thin-gate oxide films, plus give an increase of the contact resistance for via-holes of a small area. Consequently, the growth of native oxide films has received an increasing attention with a decrease of pattern dimension of integrated circuits.[1-7]

The growth of several angstrom (Å) thickness native oxide has been reported to be observed on Si surfaces exposed to air for 10 h.[3] On the contrary, the oxide thickness formed at room temperature during 10 h is estimated much below 1 Å from the growth rate activation energy determined from temperature dependence data of the thermal oxidation rate in dry or wet oxygen, i.e., the thermal oxidation data conjecture that the oxide is not grown on Si surface at room temperature. Therefore, the growth mechanism of the native oxide is considered entirely different from that of the thermal oxide. This consideration promotes researches concerning the origin of the native oxide growth.

Some interesting results for the influence of native oxide on semiconductor processing have recently been reported.[8,9] It has been demonstrated that the use of different preoxidation cleaning procedures including wet chemical cleaning of silicon surface had a significant effect on the kinetics of thermal silicon oxidation.[8] This result can be interpreted to demonstrate the influence of native oxides on the thermal oxidation kinetics. It has been pointed out, moreover, that iron ions in HNO_3 solution react with the native silicon oxide to form an Fe(III)-O complex, but do not react with silicon itself.[9] A drastic degradation of metal-oxide-semiconductor device characteristics has been observed by an increase of iron impurities in native oxides. This indicates that native oxides serve as the source of iron impurities to diffuse into the silicon and produce defects in succeeding high-temperature processes.[10-13] These characteristics have been demonstrated for various metal impurities such as iron, nickel, and chromium.[10-12] Thus the existence of native oxide film on silicon surfaces degrades the control ability of the quality of device fabrication processings and the performance and reliability of semiconductor devices themselves. Though the existence of native oxides on the silicon surfaces has been demonstrated to give severe influences on the high-quality processings, however, a method to control the native oxide growth has not yet been established.

In this paper, we describe the factors controlling the native oxide growth in air and in ultrapure water at room temperature and propose methods to control the native oxide growth.[14-18] We also discuss the structural differences between native oxides formed in various environments.

II. EXPERIMENT

The wafers used in these experiments are phosphorous (P) doped *n*-type Cz (100) wafers with a resistivity of 2–4 Ω cm (carrier concentration: 10^{15} cm^{-3}), n^+-type (10^{20} cm^{-3}) wafers, and p^+-type (10^{20} cm^{-3}) wafers, where n^+- and p^+-type layers are prepared by chemical vapor deposition of phosphosilicate glass (PSG) and borosilicate glass (BSG) followed by the thermal diffusion treatments, respectively. All wafers are chemically cleaned with $(H_2SO_4 + H_2O_2)$, $(NH_4OH + H_2O_2 + H_2O)$, and $(HCl + H_2O_2 + H_2O)$ solution, etched with $(HF + H_2O)$ solution, and then rinsed with ultrapure water with a dissolved oxygen concentration of 0.6 ppm. Most of the wafers are succeedingly dipped in hot ultrapure water (90 °C) and

[a] Present address: Tokyo Central Research Laboratory, Mitsubishi Gas Chemical Company Inc., 1-1-6 Niijuku, Katsushika, Tokyo 125, Japan.
[b] Present address: Alps Electric Co., Ltd., Furukawa, Miyagi 989-61, Japan.

 0021-8979/90/151272-10$03.00

dried with hot ultraclean argon gas blow (70–80 °C). Other remaining wafers are dried with ultraclean nitrogen gas blow (23 °C).

Native oxide film thicknesses are determined by x-ray photoelectron spectroscopy (XPS) combined with ellipsometry. Native oxide film thickness has been mainly determined by ellipsometry so far, where the thickness has been derived based on an assumption of a constant oxide refractive index such as 1.46 because an accuracy of the measurement of the refractive index degrades for thin films having a thickness less than 70 Å. But it has been recently reported that the refractive index for thermal oxides near the oxide-Si interface is different from that of bulk oxide, i.e., the refractive index of an interlayer having a thickness of 6 Å between Si and its thermal oxide is evaluated as 2.8.[19,20] It is, therefore, difficult to obtain an accurate film thickness of native oxides only by using ellipsometry. The native oxide thickness measured by ellipsometry has been demonstrated experimentally thicker than that by XPS.[3]

We propose a method to determine the thickness of very thin oxide films as follows: (1) The thickness of thermal oxide films (70–140 Å) is measured by ellipsometry without the postulation of the refractive index (see Appendix). (2) The Si_{2p} spectra of the same oxides are measured by XPS. (3) The area ratio of the signal from the oxide (SiO_x: $x \geqslant 0.5$) to that from the Si substrate is calibrated with the thickness measured by ellipsometry. The escape depths of electrons for the oxide overlayer and the Si substrate are determined. (4) The thicknesses of the native oxide films are determined from the area ratio of XPS spectrum of the native oxide and above calibration data. The minimum thickness which can be measured by ellipsometry without the assumption of the refractive index is 70 Å. The maximum thickness from which both the XPS signal from the oxide overlayer and the Si substrate can be observed for an XPS system with Al $K\alpha$ x-ray source is 140 Å. So 70–140-Å-thickness oxides are used for the thickness calibration between ellipsometry and XPS. The native oxide film thickness determined by above-described method is considered to be correct as long as the atomic density of the native oxide is equal to that of the thermal oxide, because the peak area of XPS spectrum corresponds to the number of atoms. This method gives a normalized thickness for native oxides having atomic densities different from that of the thermal oxide, where the native oxide thickness is normalized by the thermal oxide thickness. The H_2O concentration in processing gases such as oxygen and nitrogen is monitored with a dew-point meter having a lowest dew point of -110 °C. The dissolved oxygen level in ultrapure water is measured by polarography having a lowest level of 5 ppb. The amount of the dissolved Si in ultrapure water is measured by atomic absorption. The roughnesses of the native oxide surfaces and the Si wafer surfaces after removing the native oxide overlayer by ($HF + H_2O$) etching are evaluated by light beam reflection and the scanning tunneling microscopy (STM), respectively.

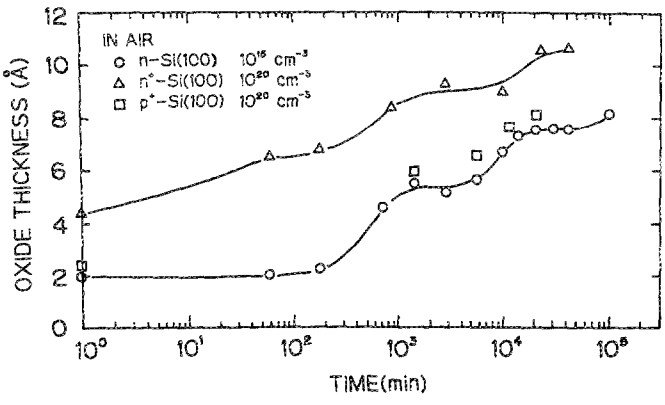

FIG. 1. Oxide thickness as a function of exposure time of wafers to air at room temperature.

III. RESULTS

A. Growth of native oxide in air

The thicknesses of native oxide films on n-, n^+-, and p^+-type Si wafers are shown as a function of exposure time to clean room air at room temperature in Fig. 1, where the clean room air is characterized by the cleanliness less than 0.000 002 (particle size greater than 0.17 μm), an average temperature of 23.7 °C, and an average humidity of 42% (where the H_2O molecule concentration is 1.2% of total air molecule concentration). It is obvious in Fig. 1 that these plots indicate an approximately successive step functionlike increase of native oxide. This can be considered to suggest that layer-by-layer oxide growth occurred on these wafers at room temperature.[5] For n-Si, it appears in Fig. 1 that the growth to 5.4 Å and the succeeding increase to 7.6 Å correspond to two molecular layers of growth followed by one additional layer of growth of the native oxide. The initial normalized thickness of native oxide on the n^+-Si wafer is 4.4 Å, while the thickness on n- and p^+-Si wafer are 1.9 and 2.3 Å, respectively. These oxides are mainly grown during rinsing with ultrapure water and water drying procedure after a diluted HF treatment. Here, it should be attended that the Si atoms contributing the initial oxide thickness determined in this measurement includes Si atoms terminated with hydrogen at Si surface. Therefore, the actual oxide thicknesses on each Si surfaces are estimated to be thinner than above thickness values at the initial stage.

The effect of H_2O concentration in air on native oxide growth is summarized in Table I. The oxide thickness is 6.7 Å after 7 days exposure to the clean room air containing 1.2% H_2O. When the moisture level is suppressed less than 0.1 ppm in ($N_2 + O_2$) environment having a concentration ratio of N_2 to O_2 as 4 to 1 and N_2 environment, the thicknesses of native oxides are 1.7 and 1.9 Å, respectively. It is worthwhile to note in Table I that the native oxide hardly grows at all even after 7 days exposure to the air when the H_2O concentration in air is suppressed less than 0.1 ppm. The bare Si surface is significantly oxidized even at room temperature in the environment of coexistence of oxygen and moisture.

TABLE I. Growth of native oxide for H_2O concentrations during 7 days.

Ambient	H_2O concentration	Oxide thickness (Å)
Air	~1.2% (Humidity: 42%RH)	6.7
O_2/N_2 (=$\frac{1}{4}$)	<0.1 ppm	1.7
N_2	<0.1 ppm	1.9

B. Growth of native oxide in ultrapure water

Figure 2 indicates the oxide thickness on n-Si wafer as a function of the immersion time in ultrapure water having different dissolved oxygen concentrations such as 0.04, 0.6, and 9 ppm at room temperature. The dissolved oxygen concentration in ultrapure water is 0.04 ppm (40 ppb), while it is increased up to 0.6 ppm in overflow rinsing situation, and up to 9 ppm in equilibrium with air at room temperature. It is seen in Fig. 2 that the oxide thicknesses increase with increasing immersion time and dissolved oxygen concentration. These curves are nearly parabolic; i.e., the native oxide growth mechanism in the ultrapure water has been confirmed different from that in the air defined by the layer-by-layer growth. This result suggests that the native oxide growth is suppressed in ultrapure water by decreasing the dissolved oxygen concentration.

Figure 3 shows the native oxide thickness on n- and n^+-Si wafers as a function of the immersion time in ultrapure water with 9-ppm dissolved oxygen concentration. The native oxide thickness (3.2 Å) on n^+-Si is initially thicker than that (1.9 Å) on n-Si. It is worthwhile to note in Fig. 3 that the native oxide thickness on n^+-Si tends to saturate at the value of 10 Å in spite of its rapid initial growth, while on

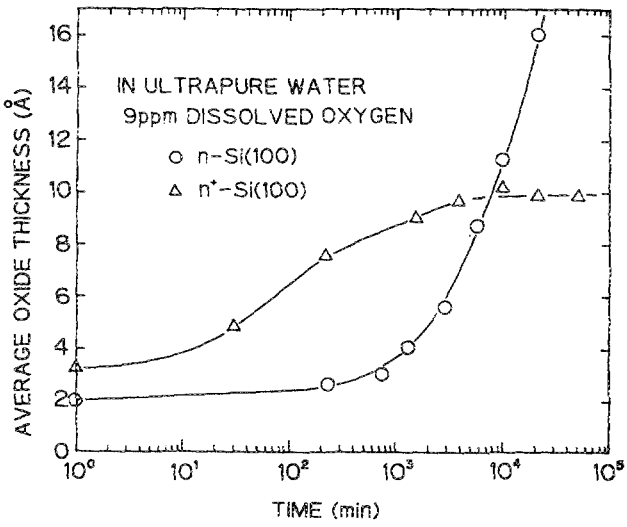

FIG. 3. Oxide thicknesses on n-Si and n^+-Si as a function of immersion time in ultrapure water with 9-ppm dissolved oxygen concentration.

n-Si, it continuously increases with an increase of the immersion time following parabolic law. This result suggests that the native oxide growth on n^+-Si is considered to come from a field-assisted mechanism.[21]

The native oxide thickness on n^+-Si is shown as a function of overflow rinsing time in Fig. 4, where the dissolved oxygen concentration in ultrapure water is 0.6 ppm and the wafer surface dry procedure is due to clean N_2 blow. The oxide thickness grown during 2-min rinsing after a diluted HF treatment is 2.6 Å, and it increases to 3.3 Å with an increase of the immersion time to 60 min. This result implies that the initial growth rate of native oxide is very high; i.e., the oxide growth on n^+-Si in ultrapure water can be interpreted by a field assist oxidation model.[21] The oxide thickness grown on n- and n^+-Si under different rinsing and drying conditions is shown in Table II. The rinsing time is kept constant at 10 min. The oxide thickness on n^+-Si becomes thin as the dissolved oxygen concentration decreases. The

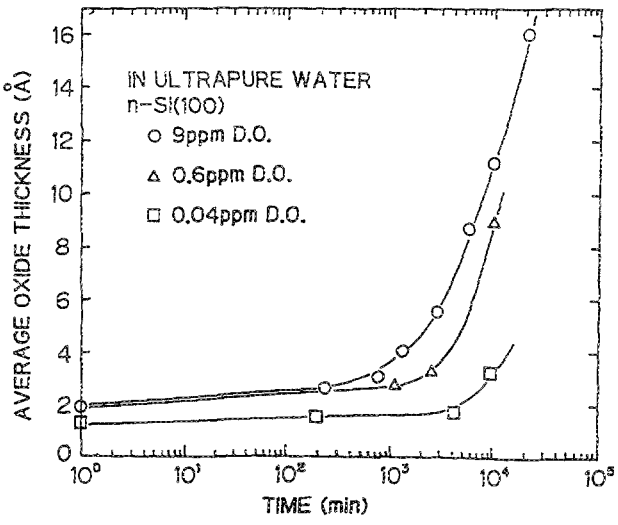

FIG. 2. Oxide thicknesses as a function of immersion time of wafers in ultrapure water at room temperature for different dissolved oxygen concentrations.

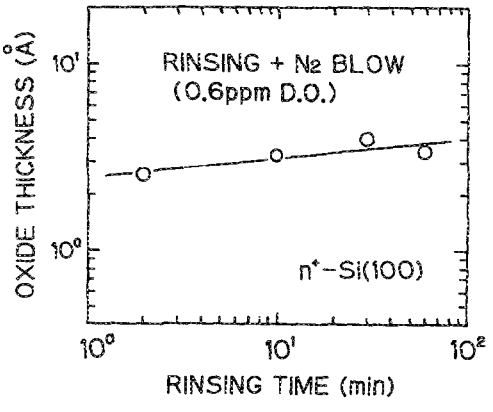

FIG. 4. Oxide thickness on n^+-Si as a function of rinsing time by overflowing ultrapure water. The dissolved oxygen concentration in ultrapure water is 0.6 ppm.

TABLE II. Growth of native oxide on n- and n^+-Si under different ultrapure water rinsing and drying.

Condition	n-Si(100)	n^+-Si(100)
Rinsing (0.04 ppm DO) + N_2 blow	1.3	2.9
Rinsing (0.6 ppm DO) + N_2 blow	1.9	3.2
Rinsing (0.6 ppm DO) + hot water dipping (1 min) + hot Ar blow	1.9	4.4

oxide thickness on n^+-Si increases for hot water dipping and hot Ar blowing. The oxide thickness (2.3 Å) grown on a p^+-Si wafer during rinsing with ultrapure water and a drying procedure after a diluted HF treatment is nearly equal to that (1.9 Å) on n-Si, as seen from Fig. 1. The average bond strength of Si—Si in p^+-Si is weak compared with that in n-Si, because p^+-Si has many holes. Therefore, this result also indicates that the native oxide growth in ultrapure water is dependent on electron concentration, but not the average strength of Si—Si bonds.

Figure 5 shows the time dependence of the numbers of Si atoms in native oxide and of Si atoms dissolved in ultrapure water, where the dissolved oxygen concentration in ultrapure water is 9 ppm and N_{Si} is defined as the number of Si atoms per unit area on wafer surface. Si dissolution occurs simultaneously during native oxide growth. The number of dissolved Si atoms is larger than the number of Si atoms in native oxide by one order of magnitude. The normalized thickness of the number (1.8×10^{16} cm^{-2}) of the dissolved Si atoms to the single-crystal Si(100) thickness and the native oxide thickness including the number of Si atoms of 9.2×10^{14} cm^{-2} are 34.9 and 4.1 Å for 1315 min (~22 h), respectively. The number of Si atoms in the native oxide film increases correspondingly with the number of dissolved Si atoms. This indicates that native oxide growth is strongly influenced by the dissolution of Si into ultrapure water.

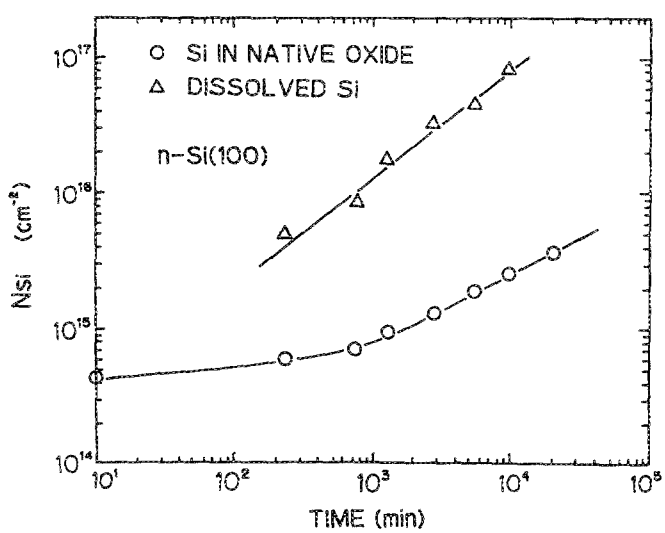

FIG. 5. Time dependence of the number of Si atoms in native oxide and the number of dissolved Si atoms in ultrapure water for wafers immersed in ultrapure water. N_{Si} is defined as the number of Si atoms per unit area on wafer surface.

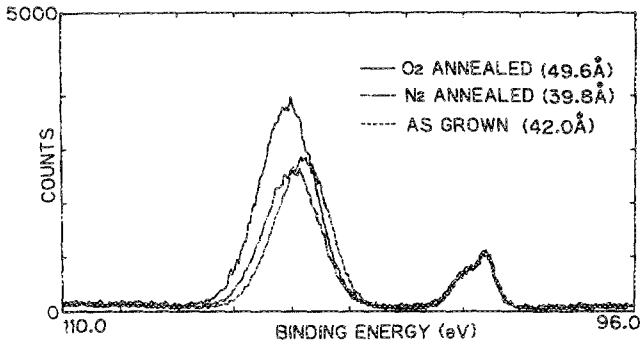

FIG. 6. Si_{2p} XPS spectra of native oxides grown in ultrapure water for 46 days and after dry O_2 annealing and dry N_2 annealing at 500 °C for 1 h.

Figure 6 shows Si_{2p} XPS spectra of the native oxide grown in ultrapure water for 46 days at room temperature and after O_2 annealing and N_2 annealing at 500 °C for 1 h. The thicknesses of as-grown oxide, O_2 annealed oxide, and N_2 annealed oxide are 42.0, 49.6, and 39.8 Å, respectively. The oxide thickness increases with O_2 annealing. This indicates that the oxidation reaction of Si at the native oxide/Si interface proceeds even at 500 °C. The slight decrease of the oxide thickness by N_2 annealing is conjectured to be due to the deoxidation of Si—O or Si—OH group, because Si_{2p} XPS data indicate that the number of Si atoms bound with O or OH decreases by N_2 annealing. The binding energy shifts for as-grown, O_2 annealed, and N_2 annealed oxide are 4.49, 4.87, and 4.72 eV, respectively. The binding energy of the native oxide becomes high by O_2 or N_2 annealing. However, the electrical property of these oxides is still leaky.

Figure 7 shows the oxide thickness on n-Si wafer as a function of the immersion time in a solution of H_2O_2 includ-

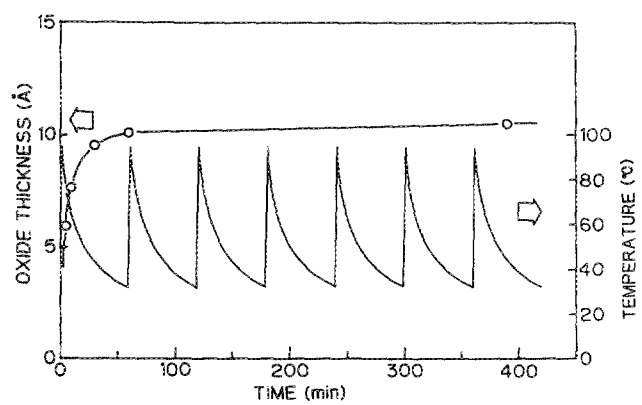

FIG. 7. Oxide thickness on n-Si as a function of immersion time in (H_2O_2 + Pt) solution.

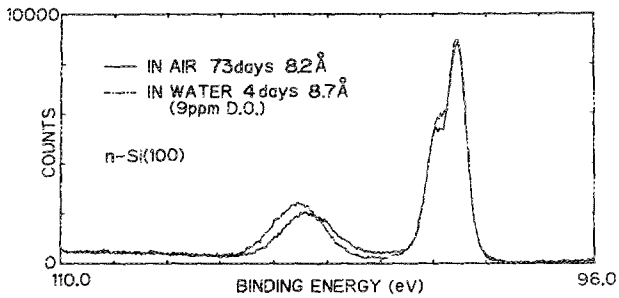

FIG. 8. Si_{2p} XPS spectra of native oxide on Si in air and in ultrapure water.

ing a mesh of Pt catalyst, where the temperature of the solution is also given as a function of the time and the solution is exchanged for a new solution every 1 h. Pt catalyst is used to produce oxygen radical from H_2O_2. The oxide thickness saturates at 10 Å even on *n*-Si wafer. This result indicates that the oxide growth mechanism in $(H_2O_2 + Pt)$ solution is different from that in ultrapure water. It is considered that the oxide growth in $(H_2O_2 + Pt)$ solution is controlled by a field assist oxidation even on *n*-Si having low electron concentration, because a number of oxygen radicals are adsorbed on the Si surface.

C. Native oxide structures

Si_{2p} XPS spectra of the native oxides grown in air and in ultrapure water are shown in Fig. 8, where the take-off angle of the photoelectron is 35°. The binding energy of SiO_x $(x > 1)$ peak for the native oxide in ultrapure water is higher than that in air. The intensity of the suboxide (SiO bond) at the oxide-Si interface for the native oxide in ultrapure water is smaller than that in air. The angular dependence plots of the area ratio of the XPS signal from SiO_x to that from Si for native oxide (15.9 Å) in ultrapure water overlapped with the plots for thermal oxide (17.7 Å). It appears that the native oxide in ultrapure water is not grown in an islandlike configuration, covering the Si substrate. The oxide-Si interface of the native oxide in ultrapure water is rough at atomic level compared with that in air, because the number of SiO bonds at the interface of the native oxide grown in ultrapure water is fewer than that in air. The roughness of the native oxide-Si interface can be observed by STM. Figure 9 shows STM profile of the Si surface right after removing the native oxide overlayer grown in ultrapure water by $(HF + H_2O)$ etching. It can be seen that the roughness of the native oxide-Si interface increases as the native oxide grows in ultrapure water. Observation of the native oxide surface with reflected white light indicated that the surface of the native oxide in ultrapure water also becomes rough with the growth of the oxide. In Fig. 8, the XPS intensity at left side shoulder of the peak from Si for the native oxide grown in ultrapure water is larger than that in air. The binding energy of the peak obtained by the subtraction of the spectrum for the native oxide in air from that in ultrapure water is nearly equal to local electronegativity model[22] for Si═H_2 and Si—H bonds. It is conjectured that the Si═H_2 and Si—H bonds exist at the

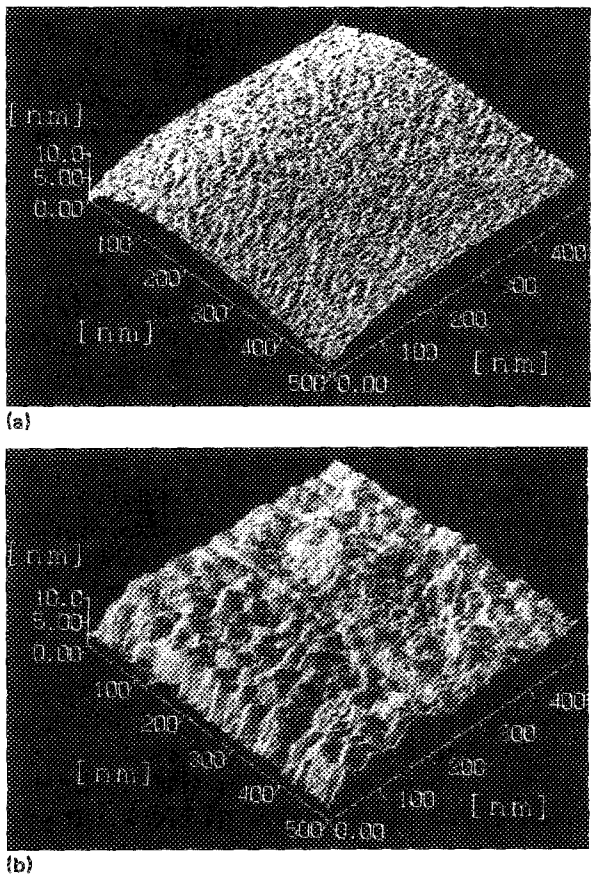

FIG. 9. STM profiles of Si surfaces (a) of cleaned wafer and (b) right after removing the native oxide grown in ultrapure water with the dissolved oxygen concentration of 9 ppm for 20 days.

interface of native oxides grown in ultrapure water.[18]

Si_{2p} XPS spectra of native oxides grown on *n*-Si by various chemical treatments are shown in Fig. 10. The intensities from SiO bond at the oxide-Si interface of the native oxides in the NH_4OH solution and in the HCl solution are smaller than that in the H_2SO_4 solution. This indicates that the interface of the native oxide in the NH_4OH solution[23] and in the HCl solution is atomically rough compared with that in the H_2SO_4 solution.

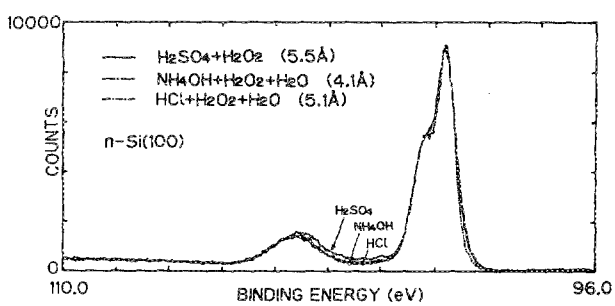

FIG. 10. Si_{2p} XPS spectra of native oxides grown on *n*-Si by various chemical treatments.

TABLE III. Native oxides under various conditions.

Sample[a]	Oxide thickness (Å)	E[b] (eV)	Contact angle (°)	Dissolved Si[c] weight ($\mu g/cm^2$)
In air 4 days	5.6	3.85	35.7	0.14 (9 days)
In ultrapure water (9 ppm DO) 2 days	5.6	4.08	11.4	4.03 (7 days)
$H_2SO_4 + H_2O_2$ cleaning	5.5	3.83	<10	<0.05 (7 days)
$NH_4OH + H_2O_2 + H_2O$ cleaning	4.1	3.99	<10	

[a] n-Si(100).
[b] $E = E - E(Si_{2p_{3/2}})$.
[c] Into ultrapure water (9 ppm DO).

The results showing the structural difference between the native oxides grown under various conditions is summarized in Table III. The binding energy of SiO_x $(x>1)$ peak for the native oxide in ultrapure water is higher than others. It is seen from the contact angle data of the ultrapure water droplet that the surface of the native oxide formed in air is close to being hydrophobic. This implies that the many Si atoms at the native oxide surface are terminated by hydrogen atoms. The amount of Si dissolved upon exposure to ultrapure water for the native oxides grown under various environments, with exception of ultrapure water, is little. This proves that the structure of the native oxide grown in ultrapure water is different from that of other oxides.

D. Growth of native oxide on HF gas etched silicon

The growth of native oxide films on clean bare silicon surface obtained in the gas phase etching technology is also investigated. The bare silicon surface etched by HF gas is covered by chemically combined fluorine, i.e., fluorine-terminated silicon surface.[24] This chemically combined fluorine give a definite influence on succeeding processes. The effect of fluorine-terminated silicon surface on succeeding processes was evaluated by the sputtering epitaxy.[25-30] Figure 11 shows reflection electron diffraction pattern from Si epitaxial film grown using rf-dc sputtering technology at a substrate temperature of 300 °C on three different silicon surfaces such as fluorine-terminated silicon surfaces, native oxide surfaces having a thickness of 7 Å ($SiO_x: x>0.5$), and wet-cleaned silicon surfaces having 0.4 Å of native oxide ($SiO_x: x>0.5$). Single-crystalline silicon is obtained only on the wet-cleaned silicon surface. An amorphous silicon film is grown even on the native oxide surface having a thickness of 7 Å, indicating that the existence of the native oxide degrades the quality of the semiconductor process, in particular, a low-temperature process. The results of this low-temperature sputtering silicon epitaxy are summarized in Table IV. The sheet resistivity of grown silicon film having a thickness of 0.2 μm on the wet-cleaned silicon surface is 100 Ω. On the other hand, the grown films are amorphous silicon having the sheet resistivity of 5×10^6 Ω on the native oxide surface and amorphous silicon having the sheet resistivity of $3-5\times10^6$ Ω on the fluorine-terminated silicon surface, when all process parameters are kept at the same conditions. Thus fluorine-terminated silicon surfaces exhibit similar characteristics to native oxide existence for film depositions.

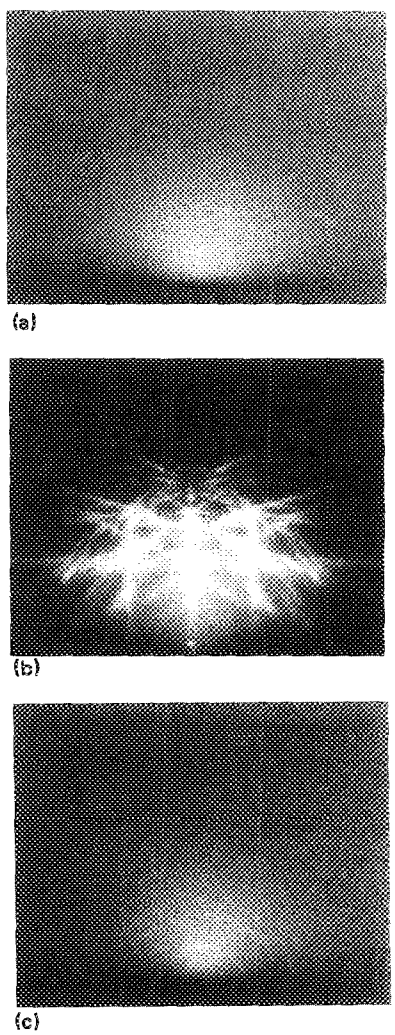

FIG. 11. Reflection electron diffraction pattern from Si epitaxial film on (a) native oxide surface having a thickness of 7 Å (before cleaning), (b) wet-cleaned silicon surface, and (c) dry-cleaned silicon surface using rf-dc sputtering.

TABLE IV. Resistivity of sputtering epitaxial silicon film.

Silicon substrate		Epitaxial silicon	
HF cleaning	SiO_x film thickness (Å) ($x>0.5$)	Crystal structure	Sheet resistivity[a] (Ω)
Before cleaning	7	amorphous	5×10^{6}
Wet cleaning	0.4	single-crystal	100
Dry cleaning	0.3	amorphous	3–5×10^{6}

[a] Sheet resistivity: Four-point probe method.

Figure 12 shows the F_{1s} XPS spectra from the fluorine-terminated surface after 1-h thermal treatment up to 930 °C in dry N_2 at atmospheric pressure. The F_{1s} spectra peak intensity does not change even after heating the substrate up 930 °C. Terminating fluorine can not be eliminated by heating silicon wafer up to 930 °C. F_{1s} XPS spectra from a fluorine-terminated silicon surface are shown for the different bombarding Ar-ion energies in Fig. 13, where the effect of the thermal treatment in an ultrahigh-vacuum environment is also given. The peak intensity of F_{1s} spectra decreases with an increase in Ar-ion energy, but the elimination of terminating fluorine is not sufficient even when the Ar-ion energy is increased up to 10 eV, as shown in the curve.

Figure 14 shows the thicknesses of native oxide films on HF acid etched and HF gas-etched Si surfaces as a function of exposure time to clean room air at room temperature, where HF gas-etched Si surfaces are prepared by a dry cleaning technology using gas-phase anhydrous hydrogen fluoride.[24] It can seen from Fig. 14 that the growth of the native oxide on HF gas-etched Si is slightly suspended in initial stage compared with that on HF acid-etched Si.

Fluorine strongly terminates silicon atoms on a wafer surface, resulting in the fact that fluorine cannot be sufficiently eliminated by the thermal treatment or the Ar-ion bombardment. Thus the fluorine termination has a protection effect of silicon surfaces against heat treatment or Ar-ion bombardment. However, the fluorine termination sufficiently cannot protect the silicon surface against the native oxide growth under the coexistence of oxygen and wafer as shown in Fig. 14. Therefore, this led us to the conclusion that the closed system in which wafers are not exposed to air is necessary in the production line in order to keep the wafer surface clean.

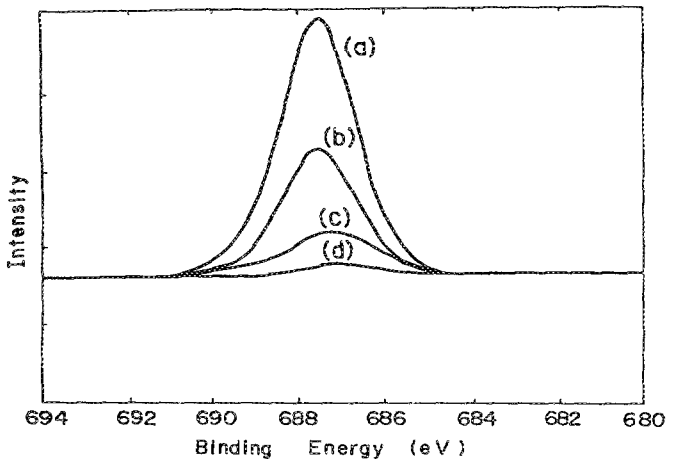

FIG. 13. F_{1s} XPS spectra from fluorine-terminated surface by low-energy Ar bombardment. Bombardment conditions are (a) no bombardment (dry-cleaned surface), (b) no bombardment (substrate temperature 300 °C, base pressure 5×10^{-9} Torr), (c) Ar-ion energy of 3 eV, substrate temperature 300 °C, Ar gas pressure 8×10^{-3} Torr, and bombarding Ar-ion energy of 10 eV, substrate temperature 300 °C, Ar gas pressure 8×10^{-3} Torr.

IV. DISCUSSION

The chemical bond of Si atoms on wet-cleaned wafer surfaces has been analyzed by some spectroscopic measurements.[31–33] Electron energy-loss spectroscopy measure-

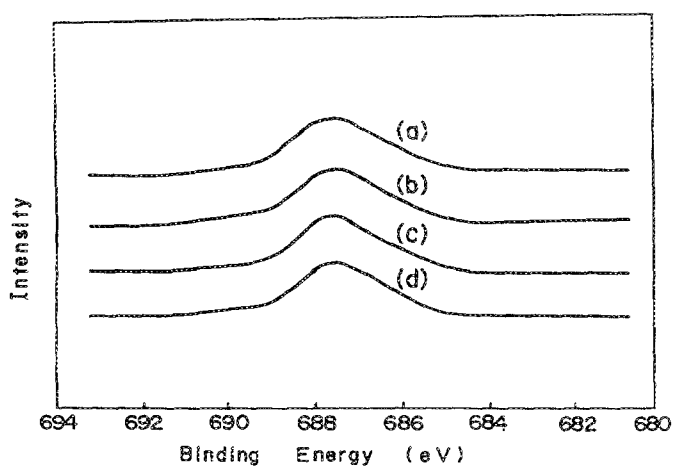

FIG. 12. F_{1s} XPS spectra from fluorine-terminated surfaces heated up to various temperatures in dry N_2 gas environment of atmospheric pressure at (a) room temperature, (b) 80 °C for 1 h, (c) 630 °C for 1 h, and (d) 930 °C for 1 h.

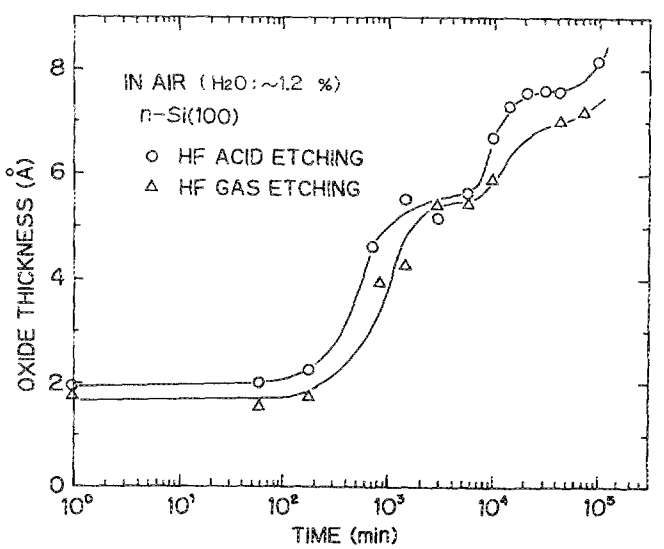

FIG. 14. Oxide thicknesses on HF acid-etched and HF gas-etched Si surfaces as a function of expose time of wafers to air at room temperature.

ments showed that an Si surface dipped into hydrofluoric acid is covered mainly by Si—H groups with a small number of Si—F bonds.[31] On the other hand, a dip of the wafer in an ammonia or HCl hydrogen peroxide/water mixture was shown to create a hydrophilic surface, caused by the formation of Si—OH groups. Fourier transform infrared spectroscopy measurements proved that the Si surface prepared with ultraviolet cleaning followed by HF dipping has a hydrogen monoatomic layer terminating the dangling bonds of Si.[32] Thermal desorption spectroscopy measurements indicated that Si surface right after a diluted HF dipping is covered primarily by H, with some H_2O or OH.[33] It can be seen from above-mentioned research results that most Si atoms at a cleaned wafer surface are terminated by hydrogen.

The oxide thickness formed at room temperature after 10-h exposure to the air is estimated around 10^{-13} Å from the extrapolation of the temperature dependence data of the oxidation rate of Si in dry or wet oxygen between 800 and 1050 °C shown in Fig. 15. It can be considered, thus, that the oxidation mechanism of Si in air at room temperature is entirely different from the thermal oxidation mechanism. The following model is proposed for the oxidation of Si at room temperature: Si atoms at a cleaned wafer surface are terminated by hydrogen. The oxygen species break Si—Si bonds to produce Si—O bonds, the remaining Si—H bonds which cause hydrophobic behavior. The oxygen species are produced at native oxide surfaces by the coexistence of O_2 and H_2O, or the Si—O bonds are produced by the coexistence of O_2 (O) and H_2O(OH) near Si—Si bonds. The Si—Si bonds of the underlayer Si are broken to produce Si—O bonds after all of the Si atoms in the overlayer are oxidized; i.e., the overlayer structure converts to the amorphous phase, resulting in layer-by-layer oxide growth. Figure 16 illustrates this oxidation scheme conceptually.

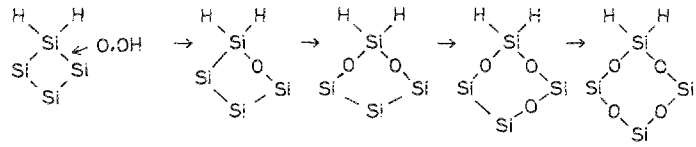

FIG. 16. A model of native oxide growth in air.

Figure 17 illustrates the chemical structure model of the native oxide grown in ultrapure water. The Si atoms of native oxide surface are terminated by O or OH. The Si—H groups exist at the oxide-Si interface.

Three models explaining Si dissolution into ultrapure water can be proposed: First, Si compounds are produced at the oxide-Si interface with the oxidation reaction of Si. These Si compounds diffuse through the native oxide and dissolve into ultrapure water. Second, the native oxide grown in ultrapure water is etched by ions and/or dissolved oxygen. Third, the Si atoms at Si surface dissolutes into ultrapure water to produce silica and this silica deposits on Si surface. It is, however, likely that the growth mechanism of native oxide in ultrapure water is complicated. Further investigation is necessary to clarify the mechanism of the native oxide growth accompanying the Si dissolution.

V. CONCLUSION

We have demonstrated that the growth of native oxide on cleaned Si wafers in air and in ultrapure water requires the coexistence of oxygen and water or moisture. The growth rate of the native oxide in air and in ultrapure water can be decreased by lowering moisture concentration in air and by lowering dissolved oxygen concentration in ultrapure water. Layer-by-layer growth of the native oxide has been

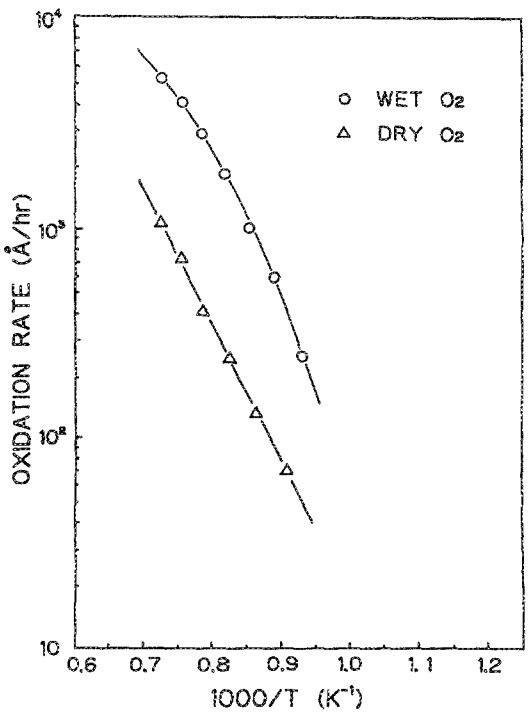

FIG. 15. Temperature dependence of thermal oxidation rate for silicon in dry and wet oxygen between 800 and 1050 °C.

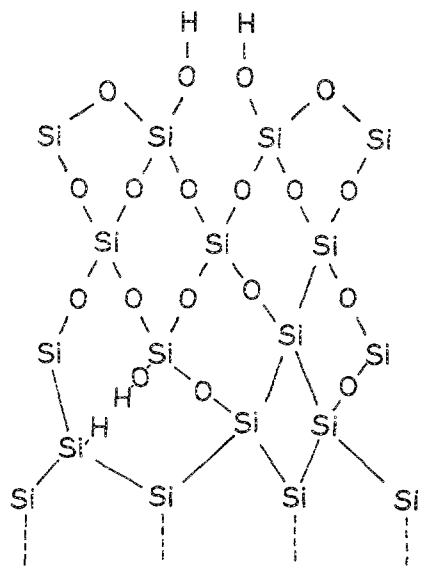

FIG. 17. A model of native oxide growth in ultrapure water.

confirmed to occur on the Si surface in air. The native oxide growth on an n-Si wafer in ultrapure water accompanies the Si dissolution into the water and degrades the atomic flatness at the oxide-Si interface, and produces a rough native oxide film surface. The growth rate of the native oxide on n^+-Si in ultrapure water is high at the initial stage and saturates at the thickness of 10 Å because of a field-assisted mechanism. The native oxide growth on n-Si in a H_2O_2 solution including a Pt catalyst is controlled by a field assist oxidation because of a number of oxygen radicals. It is found for the first time that a field assist oxidation occurs on n^+-Si in ultrapure water and on n-Si in (H_2O_2 + Pt) solution at room temperature.

We propose a nitrogen gas tunnel connecting process equipment as system to prevent native oxide growth, and an ultrapure water rinsing vessel sealed by nitrogen gas in order to suppress the native oxide growth in ultrapure water.

ACKNOWLEDGMENTS

The authors wish to thank Y. Morikage and K. Katagiri at Seiko Instruments Inc. for STM observation, Professor T. Hattori at Musashi Institute of Technology, and Dr. N. Yabumoto at NTT LSI Laboratories for useful discussions. If it is noted that preceding work of importance related to this article is not cited as a reference, it is due to our incomplete survey of reference. It would be greatly appreciated if such information or comments are provided to the authors. This study was carried out at the Super Clean Room of Laboratory for Microelectronics, Research Institute of Electrical Communication, Tohoku University.

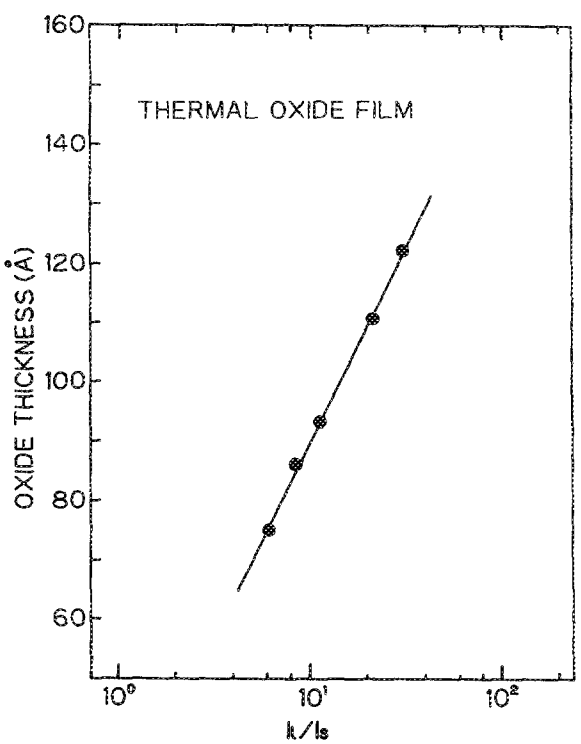

FIG. 18. Thermal oxide thickness measured by ellipsometry as a function of the area ratio of the XPS signal from the oxide (SiO_x: $x \geqslant 0.5$) to that from Si substrates.

APPENDIX

The thickness of thermal oxide films was measured by the nulling method using the ellipsometer (Shimadzu AEP-100) in the range from 70 to 140 Å. Figure 18 shows the thermal oxide thickness measured by ellipsometry as a function of the area ratio of the XPS signal from the oxide (SiO_x: $x \geqslant 0.5$) to that from the Si substrate. The accuracy of refractive indices measured in this oxide thickness region is 1.46 ± 0.01 in this ellipsometry measurement. It is seen from Fig. 18 that the oxide thickness measured by ellipsometry is not scattered as expressed by

$$d = \lambda_l \ln\left(A \frac{I_l}{I_s} + 1\right),$$

$$A = \frac{n_s \sigma_s \lambda_s}{n_l \sigma_l \lambda_l},$$

where d is the thickness of an oxide overlayer, I_s and I_l are the photoemission intensities for the Si substrate and the oxide overlayer, respectively, n_s and n_l are the densities of Si atoms, σ_s and σ_l are the atomic photoionization cross sections, and λ_s and λ_l are the escape depths. Thus the errors in refractive index and oxide thickness are considered to be small enough even for these thin films between 70 and 140 Å in our experiments.

[1] R. J. Archer, J. Electrochem. Soc. **104**, 619 (1957).
[2] F. Lukes, Surf. Sci. **30**, 91 (1972).
[3] S. I. Raider, R. Fitsch, and M. J. Palmer, J. Electrochem. Soc. **122**, 413 (1975).
[4] H. R. Philip and E. A. Taft, J. Appl. Phys. **53**, 5224 (1982).
[5] E. A. Taft, J. Electrochem. Soc. **135**, 1022 (1988).
[6] T. Hattori, K. Takase, H. Yamagishi, R. Sugino, Y. Nara, and T. Ito, Jpn. J. Appl. Phys. **28**, L296 (1989).
[7] K. Takase, T. Igarashi, N. Miyata, K. Moriki, R. Sugino, Y. Nara, T. Ito, M. Fujisawa, and T. Hattori, in Extended Abstracts of the 21st Conference on Solid State Devices and Materials, Tokyo, 1989, p. 393.
[8] G. Gould and E. A. Irene, J. Electrochem. Soc. **134**, 1031 (1987).
[9] R. Takizawa, T. Nakanishi, and A. Ohsawa, J. Appl. Phys. **62**, 4933 (1987).
[10] A. S. Maeda and M. Ogino, in Extended Abstracts of the 169th Electrochemical Society Meeting, Boston, 1986, p. 372.
[11] Y. Matsushita, in Digest, Technical Papers, 1989 VLSI Symposium, Kyoto, 1989, p. 5.
[12] Y. Matsushita, in Proceedings of the 1st Workshop on ULSI Ultra Clean Technology, Tokyo, 1989, p. 1.
[13] T. Shimono and M. Tsuji, in Proceedings of the 1st Workshop on ULSI Ultra Clean Technology, Tokyo, 1989, p. 49.
[14] T. Ohmi, Oyo Butsuri **58**, 193 (1989).
[15] T. Ohmi, M. Morita, E. Hasegawa, M. Kawakami, and K. Suma, in Extended Abstracts of the 175th Electrochemical Society Meeting, Los Angeles, 1989, p. 227.
[16] M. Morita, T. Ohmi, E. Hasegawa, M. Kawakami, and K. Suma, in Digest, Technical Papers, 1989 VLSI Symposium, Kyoto, 1989, p. 75.
[17] M. Morita and T. Ohmi, Ultra Clean Technol. **1**, 22 (1989).
[18] M. Morita, T. Ohmi, E. Hasegawa, M. Kawakami, and K. Suma, Appl. Phys. Lett. **55**, 562 (1989).
[19] E. A. Taft and L. Cordes, J. Electrochem. Soc. **126**, 131 (1979).
[20] D. E. Aspenes and J. B. Theeten, J. Electrochem. Soc. **127**, 1359 (1980).
[21] N. Cabrera and N. F. Mott, Rep. Prog. Phys. **12**, 163 (1949).
[22] G. Lucovsky, J. Phys. (Paris) Colloq. 42, C4-741 (1981).
[23] H. Mishima, T. Yasui, T. Mizuniwa, M. Abe, and T. Ohmi, IEEE Trans. Semicond. Manuf. **2**, 69 (1989).
[24] N. Miki, H. Kikuyama, I. Kawanabe, M. Miyashita, and T. Ohmi, IEEE Trans. Electron Devices **37**, 107 (1990).

[25] T. Ohmi, K. Matsudo, T. Shibata, T. Ichikawa, and H. Iwabuchi, Jpn. J. Appl. Phys. **27**, 2146 (1988).
[26] T. Ohmi, T. Ichikawa, T. Shibata, K. Matsudo, and H. Iwabuchi, Appl. Phys. Lett. **53**, 45 (1988).
[27] T. Ohmi, K. Matsudo, T. Shibata, T. Ichikawa, and H. Iwabuchi, Appl. Phys. Lett. **53**, 364 (1988).
[28] T. Ohmi, H. Iwabuchi, T. Shibata, and T. Ichikawa, Appl. Phys. Lett. **54**, 253 (1989).
[29] T. Ohmi, K. Matsudo, T. Shibata, T. Ichikawa, and H. Iwabuchi, in Extended Abstracts of the 20th Conference on Solid State Devices and Materials, Tokyo, 1988, p. 49.
[30] T. Ohmi, T. Ichikawa, and H. Iwabuchi, Appl. Phys. Lett. **54**, 523, (1989).
[31] M. Grundner and H. Jacob, Appl. Phys. A **39**, 73 (1986).
[32] T. Takahagi, I. Nagai, A. Ishitani, H. Kuroda, and Y. Nagasawa, J. Appl. Phys. **64**, 3516 (1988).
[33] N. Yabumoto, K. Minegishi, Y. Komine, and K. Sato, Jpn. J. Appl. Phys. **29**, L490 (1990).